ELASTIC-PLASTIC DYNAMIC ANALYSIS OF REACTOR BUILDINGS

by

Hajime Umemura[I] Hiroshi Tanaka[II]

SYNOPSIS

A computer program for nonlinear dynamic analysis of reactor buildings is developed. The nonlinear moment-rotation and shear stress-shear deformation characteristics of walls used in the analysis are based upon the experiments of model structures. The geometrical nonlinearity of equivalent soil spring for rocking due to foundation separation is also considered. The damping matrix in the program is formulated to accomodate the different characteristics of soil and building damping. Mathematical formulation and analytical investigation are presented.

INTRODUCTION

The reactor building of a Mark II BWR plant houses the steel primary containment which accomodates the reactor and primary coolant system. It also houses auxiliary plant facilities. The reactor building should withstand the effect of the maximum earthquake to be expected at the site, and maintain the function of supporting and accomodating structure of the important items for nuclear safety. To evaluate the dynamic behavior of a reactor building under a very strong earthquake, it is rational to include the nonlinear force deformation relationship of box and shell walls which are the major earthquake-resisting structural components of the reactor building (Fig. 1). This paper describes the nonlinear dynamic analysis of the reactor building using lumped mass models.

FORCE DEFORMATION CHARACTERISTICS OF WALLS

The experimental investigation is performed to determine the strength and force-deflection characteristics of box and conical shell type concrete walls. Four specimens as shown in Fig. 2, two box type with 1% and 1.6% reinforcement respectively (BL-10, BL-16), one conical shell type and one box and conical shell combination type with 1.6% reinforcement (CL-16, BCL-16) are each subjected to a static reversal horizontal loading cycle on upper and lower floor level. An example of the load deflection hysteresis curves obtained is shown in Fig. 3. The load deflection skeleton curve is resolved by measurement into shear and bending deformation as shown in Fig. 4. Shear deformations of BL-10 and BL-16 are shown in Fig. 5. These curves are in close agreement with Kokusho's experimental formula(1). The more complete description of the experiments is reported elsewhere(2).

In the nonlinear dynamic analysis the shear stress-shear deformation ($\tau - \gamma$) and the moment-curvature ($M - \phi$) relationships of walls are treated

I Professor, Faculty of Engineering, University of Tokyo
II Structural Engineering Division, Atomic Power Construction Department, The Tokyo Electric Power Co.

separately and tri-linear skeleton curves are assigned to the $\tau - \gamma$ and the $M - \phi$ relationships respectively. The $\tau - \gamma$ skeleton curves are the tri-linear approximation of Kokusho's formula and defined by initial shear cracking stress τ_c, second inflection point stress τ_y and ultimate shear strength τ_u. τ_c is set to be 20 Kg/cm^2 and τ_y to be 1.8 τ_c. The stiffness reduction factor β_c at $\tau = \tau_c$ and β_y at $\tau = \tau_y$ are 0.2 and 0.08 respectively (Fig. 6). The $M - \phi$ skeleton curves are defined by initial cracking moment M_c, yielding moment M_y and ultimate moment M_u as shown in Fig. 7. Initial cracking moment is calculated from

$$M_c = \left(f_r + \frac{N}{A} \right) Z_e \qquad (1)$$

where f_r is the tensile strength of concrete, N the vertical force, A the effective area of section and Z the section modulus. The yielding moment is defined as the moment associated with the initiation of yielding in the reinforcement at the extreme tension point. The $M - \phi$ skeleton curves are assigned to each member according to its sectional property and axial force. Based upon the experimental results described above and previous experimental data on shear walls and columns, origin orientated hysteresis curves for the $\tau - \gamma$ relation, and a peak orientated hysteresis curves for the $M - \phi$ relation are assumed.

MATHEMATICAL MODELS AND EQUATIONS OF MOTION

The box and cylindrical walls are treated as vertical beams (Fig. 8). Mathematical model used in the analysis is a single cantilever lumped mass model supported by rocking and horizontal spring equivalent to underlying soil (Fig. 9). Rocking spring K_θ and horizontal spring Kg associated with base contact surface are calculated by Tajimi's formula(3) assuming contact pressure distribution to be uniform for vertical load and triangular or trapezoidal for overturning moment. The horizontal spring associated with vertical contact surface of the basement is calculated by Pauw's formula(4). Geometrical nonlinearity of the soil rocking spring caused by foundation separation is represented as a tri-linear moment-rotation curve shown in Fig. 10.

The dynamic force equilibrium at each mass point of a system with non-linear stiffness is expressed at time $t+\Delta t$ as

$$\underline{M}\Delta\ddot{\underline{U}}_t + \underline{C}\Delta\dot{\underline{U}}_t + \underline{K}_t\Delta\underline{U}_t = \underline{R}_{t+\Delta t} - \underline{M}\ddot{\underline{U}}_t - \underline{C}\dot{\underline{U}}_t - \underline{F}_t \qquad (2)$$

where $\underline{M}$ and $\underline{C}$ are the mass and the damping materices; $\underline{K}t$ is the tangent stiffness matrix at time t: $\Delta\ddot{\underline{U}}t$, $\Delta\dot{\underline{U}}t$ and $\Delta\underline{U}t$ are the changes in the accelerations, velocities and displacements respectively during the time increment; $Rt+\Delta t$ is the external force vector at time $t+\Delta t$; $\ddot{\underline{U}}t$ and $\dot{\underline{U}}t$ are the accelerations and velocities respectively at time t; $\underline{F}t$ is the resisting force vector at time t. Solving the above equation using the step by step solution technique developed by Wilson et al.(5) we get

1. Umemura H., "Aseismic Design of Reinforced Concrete Building" Gihodo, 1973
2. Umemura H. et al., "Experimental Study on the Behavior of Reinforced Concrete Shear Walls Under Cyclic Loading (Part 1 and Part 2)", Annual report of Engineering Research Institute, University of Tokyo, 1975
3. Tajimi H., "Building Soil Interaction", Earthquake Engineering, Shokokusha, 1968
4. Leonards, "Foundation Engineering", McGraw-Hill 1962 PP 792-793

$$\ddot{\underline{U}}_{t+\Delta t} = (1 - \frac{3}{\theta})\ddot{\underline{U}}_t + \frac{1}{\theta}(\frac{6}{\tau^2}\Delta\underline{U}_t - \frac{6}{\tau}\dot{\underline{U}}_t) \quad (3)$$

$$\dot{\underline{U}}_{t+\Delta t} = \dot{\underline{U}}_t + \frac{\Delta t}{2}(\ddot{\underline{U}}_t + \ddot{\underline{U}}_{t+\Delta t}) \quad (4)$$

$$\underline{U}_{t+\Delta t} = \underline{U}_t + \Delta t\dot{\underline{U}}_t + \frac{\Delta t^2}{6}(\ddot{\underline{U}}_{t+\Delta t} + 2\ddot{\underline{U}}_t) \quad (5)$$

where $\tau = \theta\Delta t$ and θ is taken to be 1.4. $\Delta\underline{U}t$ is determined from

$$\underline{K}_t^* \Delta\underline{U}_t = \underline{R}_t^* \quad (6)$$

where

$$\underline{K}_t^* = \underline{K}_t + \frac{6}{\tau^2}\underline{M} + \frac{3}{\tau}\underline{C} \quad (7)$$

$$\underline{R}_t^* = \underline{R}_t + \theta(\underline{R}_{t+\Delta t} - \underline{R}_t) - \underline{F}_t + \underline{M}(\frac{6}{\tau}\dot{\underline{U}}_t + 2\ddot{\underline{U}}_t) + \underline{C}(2\dot{\underline{U}}_t + \frac{\tau}{2}\ddot{\underline{U}}_t) \quad (8)$$

The damping matrix is contrived to deal with the different characteristics of damping for the building and supporting soil. From the damping ratios assigned to the soil and to each of the structural members, the modal damping ratio for the jth mode is calculated based on the energy evaluation method[6,7] as

$$\varepsilon_j = \sum_{i=1}^{n} h_i\, {}_jW_i \Big/ \sum_{i=1}^{n} {}_jW_i \quad (9)$$

where hi is the damping ratio of member i. jWi is determined from

$${}_jW_i = \frac{1}{2}\, {}_j\underline{\Phi}_i^T \underline{k}_i\, {}_j\underline{\Phi}_i$$

where ${}_j\underline{\Phi}_i$ is the nodal displacements of member i associated with jth mode shape and $\underline{k}_i$ is the element stiffness matrix of the member.

The damping matrix is obtained from these modal damping ratios using Penzien-Wilson's approach as

$$\underline{C} = \underline{M}\,\underline{\Phi}\,\underline{\zeta}\,\underline{\Phi}^T\underline{M} \quad (10)$$

where $\underline{\Phi}$ is the mode shape matrix and $\underline{\zeta}$ is the diagonal matrix of elements ζ_j given as

$$\zeta_j = 2\varepsilon_j\omega_j / M_j \qquad (j = 1,2 \ldots\ldots m) \quad (11)$$

Mj is the generalized mass and ω_j is the circular frequency for the jth mode. The damping matrix manipulated in this way does not cause unnecessarily high damping for frequency components higher than the fundamental frequency of the system.

The displacement force relationship of a beam element as shown in Fig. 8 is

$$\underline{S} = \underline{k}_t(\underline{u} - \underline{u}_e) + \underline{f} \quad (12)$$

where $\underline{S}$ is a set of forces acting on a beam; $\underline{U}$, the displacements corresponding to $\underline{S}$; $\underline{u}_e$ and $\underline{f}$, the displacements and forces respectively at the time of last stiffness change. The tangent stiffness matrix $\underline{k}_t$ of an element is given as

---

5. Wilson E.L. et al., "Nonlinear Dynamic Analysis of Complex Structures", Earthquake Engineering and Structural Dynamics, Vol. I, 1972
6. Whitman R.V., "Soil-Structure Interaction", Seismic Design for Nuclear Power plants, MIT Press, 1970
7. Fukasawa et al., "A Numerical Method to Determine the Damping Factors" Preprint to JSME No. 730-3, 1973

$$\underline{k}_t = \frac{EI_e}{\ell(1+\Phi_y)} \begin{bmatrix} 12/\ell^2 & & & \\ -6/\ell & 4+\Phi_y & \text{Symm} & \\ -12/\ell^2 & 6/\ell & 12/\ell^2 & \\ -6/\ell & 2-\Phi_y & 6/\ell & 4+\Phi_y \end{bmatrix} \tag{13}$$

where $\phi_y = 12\ EIe/GAe\ \ell^2$ (14)

Tangent stiffness is controlled by effective sectional area Ae and effective area moment of inertia Ie so as to maintain the force-deformation relationships assigned to each element.

NUMERICAL EXAMPLES

The first example is the comparison of elastic and inelastic analysis. Input earthquakes are El Centro 1940 NS and Hachinohe 1968 EW, normalized maximum acceleration being 500 Gal. The damping ratios are assumed to be 5% for the building and 10% for the supporting soil. Response time histories and hysteresis curves of some of the members are shown in Fig. 11. Maximum, displacements, shear forces and overturning moments are shown in Fig. 12.

The second example is the effect of maximum acceleration on the response. Input earthquake is El Centro. Maximum accelerations vary from 200 Gal to 1,000 Gal. Soil damping ratio is 15% and other conditions are the same as above. The results are shown in Fig. 13.

Parametric analyses are performed to evaluate the effect of the variations of soil stiffness. Eight earthquakes of different character including El Centro, Taft, Hachinohe, Hamaoka[8] and Hiroo[9] are used for the analyses. The maximum accelerations of these input earthquakes are normalized to 200 Gal and 500 Gal. The results are shown in Fig. 14 and Fig. 15. The complete descriptions are reported in the reference[10].

CONCLUSIONS

This paper has presented the anlytical method of the dynamic behavior of a reactor building under very strong earthquakes considering the nonlinear stiffness of the building based on the experimental results of model structures. Analytical investigation shows that the maximum shear stress and overturning moment obtained by nonlinear analysis, are smaller in the middle and lower portion of the building and may be larger in the upper portion compared with the results of elastic analysis. From the parameter study using 8 earthquakes, the standard deviations of the maximum response in each portion of the building are approximately 10 - 20%. As soil becomes harder the standard deviations of the maximum response in the upper portion increase and the standard deviations in the lower portion decrease. The effect of the parameter change is smaller in nonlinear analysis than in linear analysis.

---

8. NS component of ground acceleration recorded at Hamaoka May 9, 1974
9. EW component of ground acceleration recorded at Hiroo Jan. 21, 1970
10. Tanaka H. "Elastic-Plastic Dynamic Analysis of Reactor Buildings", Thesis presented to the Tokyo University April 1975

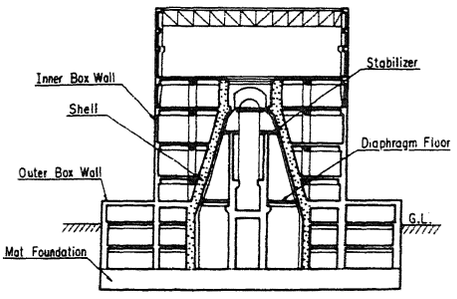

Fig. 1 Structural layout of a reactor building

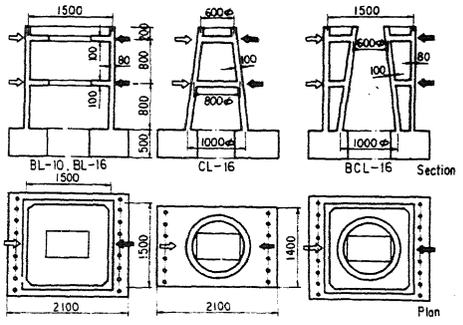

Fig. 2 Box and shell wall test specimens

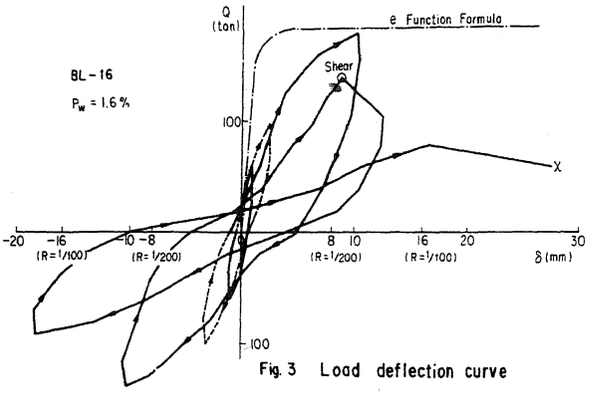

Fig. 3 Load deflection curve

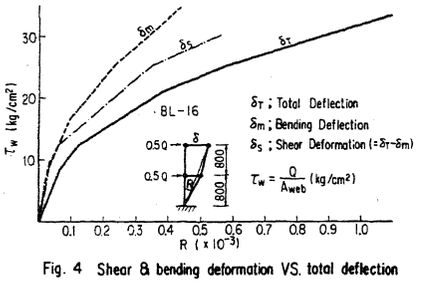

Fig. 4 Shear & bending deformation VS. total deflection

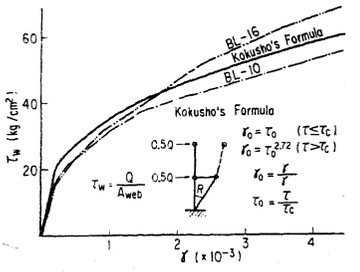

Fig. 5 Shear deformation of lower portion

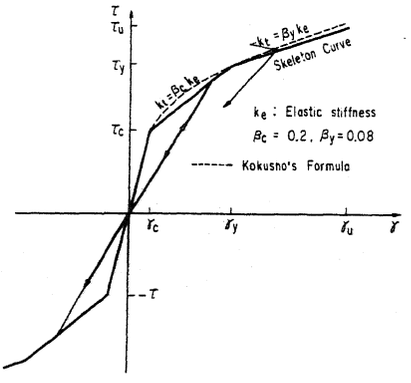

Fig. 6 τ-γ relation hysteresis curve

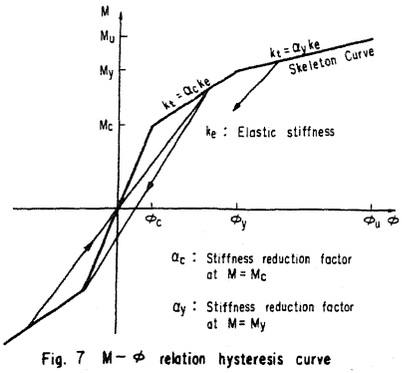

Fig. 7 M-φ relation hysteresis curve

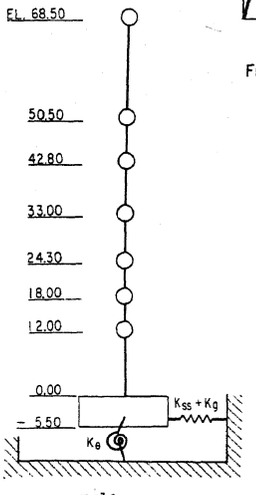

Fig. 9 Mathematical model

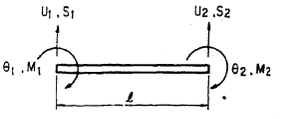

Fig. 8 Beam element

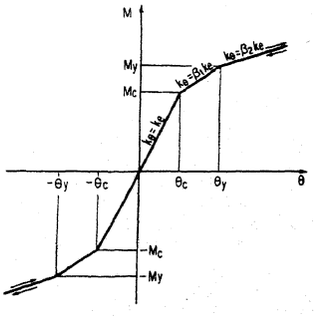

Fig. 10 Moment rotation relation of soil spring

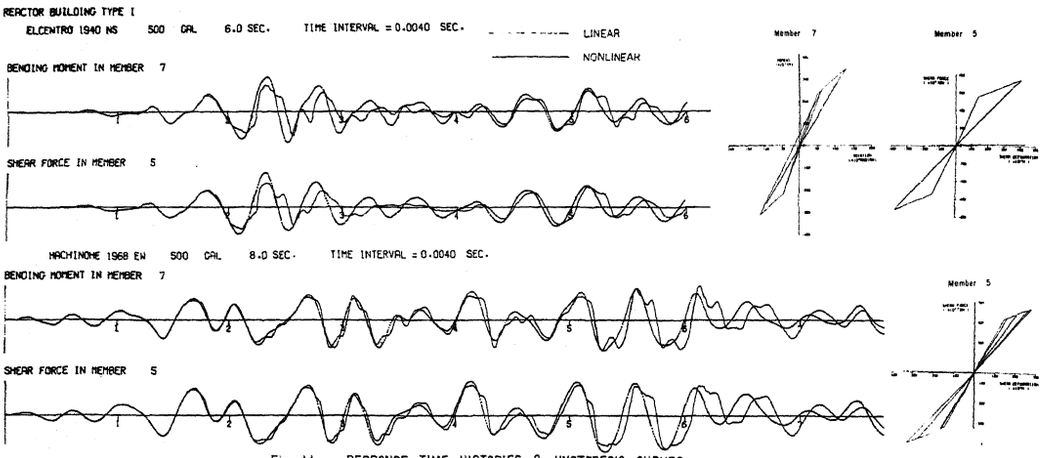

Fig. 11 RESPONSE TIME HISTORIES & HYSTERESIS CURVES

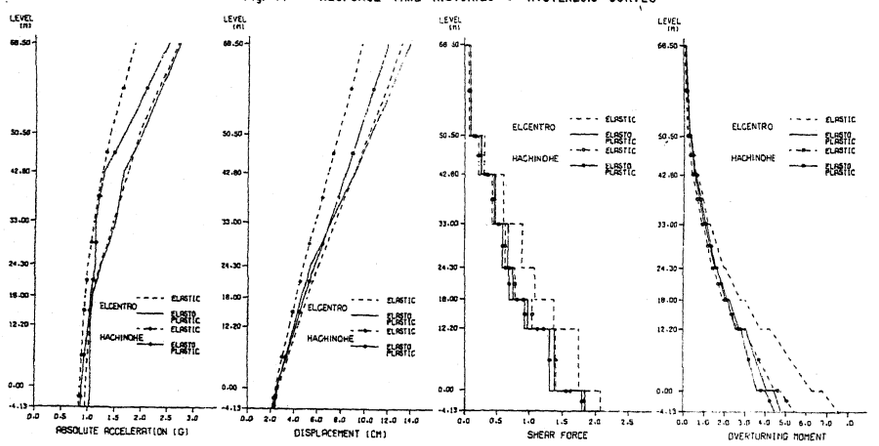

Fig. 12 MAXIMUM ELASTIC & NONLINEAR RESPONSE

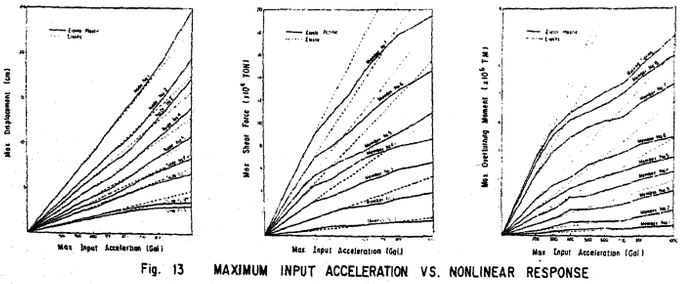

Fig. 13 MAXIMUM INPUT ACCELERATION VS. NONLINEAR RESPONSE

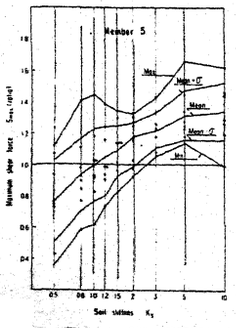

Fig. 14 SOIL STIFFNESS & MAXIMUM SHEAR FORCE (200 Gal.)

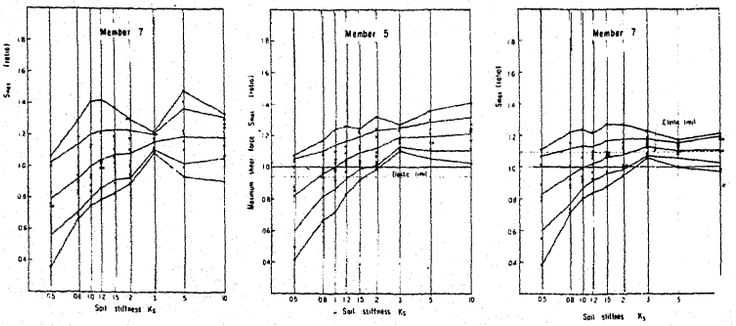

Fig. 15 SOIL STIFFNESS & MAXIMUM SHEAR FORCE (500 Gal.)